Ground state properties of odd-Z superheavy nuclei

Zhongzhou Ren,[1,2,*] Ding-Han Chen,[1] Fei Tai,[1] H. Y. Zhang,[3] and W. Q. Shen[3]
[1]*Department of Physics, Nanjing University, Nanjing 210008, People's Republic of China*
[2]*Center of Theoretical Nuclear Physics, National Laboratory of Heavy-Ion Accelerator at Lanzhou, Lanzhou 730000, People's Republic of China*
[3]*Shanghai Institute of Nuclear Research, Shanghai 201800, People's Republic of China*
(Received 21 January 2003; published 5 June 2003)

The ground state properties of odd-Z superheavy nuclei in the mass range of $Z=97-115$ and $N=140-190$ are systematically investigated in deformed relativistic mean-field (RMF) theory. Special emphasis is placed on nuclear shell effect around $N=184$. Calculations clearly show that the RMF model can reliably reproduce the data of binding energy and α decay energy of known nuclei and can also be used to predict the binding energy of unknown nuclei. It is found that deformation plays an important role for many superheavy nuclei. For $N=184$ isotones, the lighter ones are approximately spherical but the heavier ones are deformed. The α-decay energies of $N=184$ isotones are lower than those of neighboring nuclei in some cases and higher in other cases. This demonstrates that there is a complicated structural behavior for $N=184$ isotones.

DOI: 10.1103/PhysRevC.67.064302 PACS number(s): 27.90.+b, 21.10.Dr, 21.10.Tg, 21.60.Jz

I. INTRODUCTION

Since the prediction of the existence of superheavy islands in 1960s, the synthesis of superheavy elements has been a hot point in nuclear physics. Recent productions of the elements $Z=110-112$, 114, 116 [1–8] further promote the development of this field. Some important data on the structure of heavy nuclei such as α-decay energy, deformation, subshell structure, and isomers are available now [9–14]. These measurements show that nuclei having $Z\approx100$ and $N\approx152$ have ground state deformation of $\beta_2\approx0.3$ [11,12]. For nuclei having $Z\approx108$ and $N\approx162$, it is believed that deformation will lead to a subshell and the lifetime of these nuclei can be longer than expected [4]. Theoretical calculations of some even-even nuclei in this mass range also suggest that these nuclei can be deformed [15–19]. Therefore deformation cannot be neglected for theoretical studies of superheavy nuclei in order to predict reliably the properties of superheavy nuclei and to investigate nuclear shell structure. Very recently, we systematically calculated the properties of even-Z superheavy nuclei in the relativistic mean-field (RMF) model and tested the validity of this model [20,21]. For the completeness of researches we report on a systematic study of odd-Z superheavy nuclei in this paper. We also extend our calculations from known nuclei to unknown nuclei having $Z\approx113$ and $N\approx184$. These include the nuclei with proton number $Z=97-115$ and neutron number $N=140-190$. It goes without saying that this is a rather time-consuming calculation in computers due to the complex structure of superheavy nuclei. This systematic calculation is necessary in order to see the global behavior of a model.

This paper is organized in the following way. The numerical results and discussion are given in Sec. II. Section III presents a summary of this work.

*Electronic address: zren@nju.edu.cn; zren99@yahoo.com

II. NUMERICAL RESULTS AND DISCUSSIONS OF ODD-Z SUPERHEAVY NUCLEI

As this is a continuation of our study on superheavy nuclei [20,21], here we briefly review the main ideas of the RMF model. In the RMF approach, we start from a local Lagrangian density for interacting nucleons, σ, ω, and ρ mesons, and photons [22–33]. Under the mean-field approximation, we have a set of coupled RMF equations to describe the static properties of nuclei [21]. By solving these coupled equations we obtain the wave function, the binding energy, and the quadrupole deformation parameters of nuclei [21]. In the present calculations we do not include the contribution of spacial vector current of ω_μ and ρ_μ^a for odd-A superheavy nuclei because we are only interested in the average properties of nuclei such as binding energies and deformation. This approximation is reasonable for average quantities of superheavy nuclei.

We carry out RMF calculations with two sets of force parameters, TMA [18] and NLZ2 [22]. They are typical forces in the RMF model. The method of oscillator basis expansions [18,25,27–29,31] is used in solving the coupled RMF equations. The number of bases is chosen as $N_f=N_b=20$. This space is enough for the calculations here. The inputs of pairing gaps are $\Delta_n=\Delta_p=11.2/\sqrt{A}$ MeV, and this is a standard input in nuclear structural calculations. We do not make any adjustments on the current force parameters or on the pairing gaps. An axial deformation is assumed in calculations. For the details of calculations, please see the relevant papers, Refs. [21,25,27,18,29]. The quantities that we calculate are binding energies, quadrupole deformation parameters, α-decay energies, and matter root-mean-square radii of nuclear density distributions.

In our numerical calculations two approximations are made in order to simplify the computational problem and to save computational time in computers. One is that the contribution of the vector current to the binding energy of odd-A nuclei is omitted in the RMF model. It is known that this is a very small quantity and its effect on average quantities

TABLE I. The binding energies, α-decay energies, and deformations of odd-even Bk isotopes with TMA and NLZ2. Columns 2–5 are the RMF results with TMA, and columns 6–9 are those with NLZ2.

Nuclei	B (MeV)	Q_α	β_n	β_p	B (MeV)	Q_α	β_n	β_p	B(Expt.) (MeV)	Q_α(Expt.)
^{237}Bk	1786.15	10.12	0.24	0.25	1783.79	7.60	0.27	0.29	1783.80#	7.500#
^{239}Bk	1800.97	7.63	0.24	0.26	1798.70	7.24	0.29	0.30	1798.79#	7.20#
^{241}Bk	1815.21	6.20	0.25	0.26	1812.72	7.18	0.30	0.31	1813.20#	6.86#
^{243}Bk	1828.84	5.92	0.26	0.27	1826.11	6.89	0.30	0.31	1826.79	6.87
^{245}Bk	1841.84	5.72	0.27	0.28	1839.00	6.36	0.31	0.32	1839.78	6.45
^{247}Bk	1853.93	5.89	0.27	0.27	1850.94	6.29	0.31	0.32	1852.25	5.89
^{249}Bk	1865.51	5.36	0.26	0.26	1861.84	6.50	0.31	0.31	1864.03	5.53
^{251}Bk	1876.58	4.84	0.26	0.26	1872.23	6.25	0.31	0.31	1874.79	5.57#
^{253}Bk	1886.72	4.99	0.25	0.25	1882.54	5.55	0.30	0.30	1885.36#	
^{255}Bk	1896.50	4.77	0.23	0.23	1892.70	4.97	0.29	0.29		
^{257}Bk	1906.29	4.59	0.22	0.22	1902.37	4.75	0.28	0.28		
^{259}Bk	1915.86	4.31	0.21	0.20	1911.41	4.73	0.26	0.27		
^{261}Bk	1925.12	4.23	0.19	0.19	1920.08	4.44	0.24	0.25		
^{263}Bk	1934.17	3.95	0.14	0.13	1928.71	4.14	0.22	0.22		
^{265}Bk	1943.89	3.69	−0.12	−0.11	1937.20	4.03	−0.18	−0.16		
^{267}Bk	1953.42	3.35	−0.13	−0.12	1946.73	2.96	−0.16	−0.15		
^{269}Bk	1962.41	3.31	−0.13	−0.11	1955.89	2.89	−0.15	−0.14		
^{271}Bk	1970.51	3.64	−0.11	−0.11	1964.72	2.84	−0.13	−0.12		
^{273}Bk	1978.36	3.52	−0.10	−0.09	1973.45	2.62	−0.11	−0.11		
^{275}Bk	1985.90	3.49	−0.09	−0.08	1981.77	2.73	−0.10	−0.09		
^{277}Bk	1992.67	3.88	−0.06	−0.06	1989.40	3.09	−0.06	−0.07		
^{279}Bk	1999.15	4.05	−0.00	−0.00	1996.84	3.22	0.00	0.00		
^{281}Bk	2005.79	4.27	0.00	−0.00	2004.50	3.64	0.00	−0.00		
^{283}Bk	2010.48	5.84	0.00	−0.00	2008.85	6.58	−0.00	0.00		
^{285}Bk	2015.40	4.95	−0.04	−0.06	2013.05	6.21	−0.04	−0.06		
^{287}Bk	2019.90	3.85	0.05	0.07	2018.40	3.40	0.10	0.11		

such as binding energy, decay energies, and deformations can be omitted. The other is that we do not exactly include the blocking effect of odd proton because we are only interested in the average quantities of the ground state. We assume that α decay is a favored transition between the ground state of mother nuclei and the ground state of daughter nuclei. This approximation is often used in calculations of superheavy nuclei. Without these simplifications and approximations, the numerical calculation will be very difficult for a systematical study of many superheavy nuclei in deformed RMF model.

A. Binding energies, α-decay energies, and deformations of odd-A Bk and Es isotopes

Binding energies are important quantities of nuclei and they are directly related to the stability of nuclei and to α-decay energies. Whether a model can quantitatively reproduce the experimental binding energy is a crucial criterion to judge the validity of the model for superheavy nuclei. At first, let us make a detailed comparison on theoretical binding energies and experimental ones of $Z=97$–115 isotopes. We calculate the total binding energy B and the average binding energy of nucleons (B/A) for odd-A nuclei on the isotope chain of $Z=97$–115. The theoretical binding energy, quadrupole deformation parameters of protons and neutrons, and the α-decay energy are listed in Tables I–IX, together with the available data of the binding energy and α-decay energy. The variation of the average binding energy with nucleon number of some isotopes is drawn in Figs. 1 and 2.

The RMF results of odd-A nuclei on Bk and Es isotopic chains with TMA and NLZ2 are listed in Tables I and II. In Table I the first column marks the isotope. Columns 2–5 correspond to numerical results of TMA and columns 6–9 correspond to numerical results of NLZ2. B (MeV) is the theoretical binding energy. The symbols β_n and β_p in Table I denote the quadrupole deformations of neutrons and protons, respectively. Further, the symbol Q_α is the calculated α-decay energy. The experimental binding energy and α-decay energy are listed in the last two columns of the table. Experimental binding energies are obtained from the nuclear mass table [34] and the experimental α-decay energies can be deduced accordingly.

The neutron numbers of nuclei in Table I vary from $N=140$ to $N=190$. This is a wide range of this isotope chain and all known data of binding energies of odd-A nuclei are covered in our calculation. It is seen from Table I that the theoretical binding energies with both TMA and NLZ2 are very close to the experimental data. The data with symbol # are the estimated values by Audi *et al.* [34] according to the trend of the experimental data. The average deviation be-

TABLE II. The binding energies, α-decay energies, and deformations of odd-even Es isotopes with TMA and NLZ2. Columns 2–5 are the RMF results with TMA, and columns 6–9 are those with NLZ2.

Nuclei	B (MeV)	Q_α	β_n	β_p	B (MeV)	Q_α	β_n	β_p	B(Expt.) (MeV)	Q_α(Expt.)
^{239}Es	1791.20	8.60	0.23	0.24	1788.03	8.58	0.27	0.28		
^{241}Es	1806.81	7.64	0.24	0.25	1803.67	8.42	0.28	0.30	1803.83#	8.26#
^{243}Es	1821.81	7.47	0.25	0.26	1818.52	8.48	0.29	0.30	1819.02#	8.07
^{245}Es	1836.29	7.21	0.26	0.27	1832.90	8.11	0.30	0.31	1833.59#	7.91
^{247}Es	1850.13	7.01	0.27	0.27	1846.80	7.61	0.30	0.31	1847.56#	7.49#
^{249}Es	1863.24	6.90	0.26	0.27	1859.72	7.58	0.31	0.31	1861.14#	6.94#
^{251}Es	1875.77	6.46	0.26	0.27	1871.60	7.65	0.31	0.31	1873.95	6.60
^{253}Es	1887.70	6.10	0.26	0.27	1882.96	7.18	0.30	0.31	1885.58	6.74
^{255}Es	1898.56	6.31	0.26	0.26	1894.19	6.34	0.30	0.30	1896.65	6.44
^{257}Es	1908.88	6.14	0.24	0.25	1905.21	5.63	0.29	0.29	1907.48#	6.17#
^{259}Es	1919.27	5.53	0.22	0.23	1915.62	5.37	0.28	0.29		
^{261}Es	1929.39	5.19	0.22	0.22	1925.37	5.30	0.27	0.28		
^{263}Es	1939.15	5.01	0.20	0.20	1934.45	5.26	0.26	0.26		
^{265}Es	1948.55	4.86	0.16	0.16	1943.34	5.04	0.23	0.24		
^{267}Es	1957.82	4.65	0.13	0.13	1952.12	4.89	0.21	0.22		
^{269}Es	1967.80	4.39	−0.14	−0.13	1961.61	3.88	−0.16	−0.17		
^{271}Es	1977.36	4.36	−0.14	−0.13	1971.20	3.84	−0.16	−0.16		
^{273}Es	1986.15	4.56	−0.15	−0.14	1980.37	3.82	−0.14	−0.14		
^{275}Es	1994.17	4.64	−0.12	−0.12	1989.47	3.55	−0.13	−0.13		
^{277}Es	2002.23	4.44	−0.12	−0.11	1998.19	3.56	−0.11	−0.11		
^{279}Es	2009.83	4.38	−0.12	−0.12	2005.95	4.11	−0.08	−0.09		
^{281}Es	2016.45	4.52	−0.12	−0.12	2013.52	4.18	−0.05	−0.06		
^{283}Es	2022.61	4.84	−0.09	−0.09	2020.96	4.18	−0.00	0.00		
^{285}Es	2028.59	5.50	−0.08	−0.09	2025.87	6.94	−0.00	−0.00		
^{287}Es	2033.95	4.83	0.06	0.08	2031.77	5.38	0.07	0.09		
^{289}Es	2039.73	3.97	0.07	0.09	2038.09	3.26	0.11	0.13		

tween the theoretical binding energy and the experimental one is approximately 2.0 MeV. The relative deviation is approximately 0.1%. This deviation is very small. It is concluded that the RMF model can precisely reproduce the data of binding energies. This precision is achieved in calculations without any additional adjustment on force parameters or on pairing gaps.

When we compare the two sets of RMF results with TMA and NLZ2 in Table I, we see that they are very close. The average difference of binding energies between TMA and NLZ2 is approximately 2 MeV. This is a small number as it is compared with the total binding energy around 1800 MeV. This shows that the RMF model is very stable even for nuclei with a large neutron number $N=190$. This is also true for other nuclei. The global variation of average binding energies with nucleon number is drawn in Fig. 1 where the four sets of results, i.e., Bk, Es, Md, Lr, are plotted. In Fig. 1, the black points are experimental data. Two sets of theoretical results are represented by hollow triangles and hollow squares. Each set of theoretical results is connected by a solid curve. Figure 1(a) is for Bk and Es isotopes and Fig. 1(b) is for Md and Lr isotopes. The agreement between the model and the data is very impressive. It is interesting to note that the RMF results with TMA overestimate the data a little, and those of NLZ2 underestimate the data a little. The experimental data are known in a narrow window that is set by two sets of RMF results. This is useful for the prediction of unknown binding energies.

After we compare the theoretical binding energies with experimental ones, we are back to Table I again to see the variation of quadrupole deformation with nucleon number. For Bk isotopes, the RMF model predicts that there is prolate deformation from ^{237}Bk ($N=140$) to ^{263}Bk ($N=166$). The quadrupole deformation parameter with TMA is $\beta_p \approx \beta_n = 0.28$–$0.13$, and that with NLZ2 is $\beta_p \approx \beta_n = 0.32$–$0.22$. This qualitatively agrees with the measurements that nuclei having $Z \approx 100$ and $N \approx 152$ have ground state deformation of $\beta_2 \approx 0.3$ [11,12,35]. In general, the deformation parameters with two sets of RMF forces are very close, and those with NLZ2 is slightly larger than those with TMA. The variation of quadrupole deformation parameters with nucleon number is very similar for two sets of forces. There is a maximum deformation for the nuclei around $N=152$, and this corresponds to the deformed subshell of heavy nuclei. Then the prolate deformation decreases with the increase of neutron number in Bk isotopes. The prolate deformation changes to a small value for ^{263}Bk ($N=166$). From ^{265}Bk ($N=168$) to ^{275}Bk ($N=176$) a small oblate deformation appears due to the shape coexistence of nuclei, and it decreases with the increase of neutron number. Around ^{281}Bk ($N=184$) the nuclei are approximately spherical, which can

TABLE III. The binding energies, α-decay energies and deformations of odd-even Md isotopes with TMA and NLZ2. Columns 2–5 are the RMF results with TMA, and columns 6–9 are those with NLZ2.

Nuclei	B (MeV)	Q_α	β_n	β_p	B (MeV)	Q_α	β_n	β_p	B(Expt.) (MeV)	Q_α(Expt.)
^{241}Md	1794.15	9.08	0.22	0.23	1790.62	9.53	0.26	0.28		
^{243}Md	1810.63	8.86	0.22	0.23	1807.14	9.19	0.28	0.30		
^{245}Md	1826.31	8.80	0.23	0.24	1822.99	8.98	0.29	0.30		
^{247}Md	1841.53	8.58	0.25	0.26	1838.45	8.36	0.30	0.31	1838.50#	8.82#
^{249}Md	1856.26	8.33	0.27	0.27	1853.41	7.80	0.30	0.31	1853.43#	8.46#
^{251}Md	1870.30	8.13	0.26	0.27	1867.32	7.78	0.30	0.31	1867.83#	8.02#
^{253}Md	1883.94	7.60	0.26	0.27	1880.24	7.78	0.30	0.31	1881.73#	7.71#
^{255}Md	1896.89	7.18	0.26	0.27	1892.59	7.31	0.30	0.31	1894.33	7.91
^{257}Md	1908.52	7.49	0.26	0.27	1904.71	6.55	0.30	0.30	1906.32	7.56
^{259}Md	1919.78	7.08	0.21	0.21	1916.53	5.97	0.29	0.30	1917.84#	7.11#
^{261}Md	1930.69	6.49	0.21	0.21	1927.62	5.89	0.28	0.29	1929.20#	6.58#
^{263}Md	1941.38	6.19	0.21	0.21	1938.10	5.82	0.27	0.28		
^{265}Md	1951.78	5.91	0.20	0.20	1947.65	6.01	0.26	0.28		
^{267}Md	1961.76	5.69	0.18	0.18	1956.76	5.99	0.24	0.26		
^{269}Md	1971.25	5.61	0.16	0.16	1965.89	5.75	0.22	0.24		
^{271}Md	1980.84	5.29	0.12	0.13	1974.97	5.45	−0.18	−0.18		
^{273}Md	1990.96	5.14	−0.15	−0.15	1985.09	4.83	−0.17	−0.17		
^{275}Md	2000.61	5.06	−0.17	−0.16	1994.68	4.82	−0.15	−0.15		
^{277}Md	2009.18	5.27	−0.16	−0.15	2004.21	4.46	−0.13	−0.14		
^{279}Md	2017.51	4.96	−0.14	−0.14	2013.40	4.37	−0.12	−0.13		
^{281}Md	2025.68	4.84	−0.13	−0.13	2021.40	5.09	−0.09	−0.10		
^{283}Md	2033.10	5.03	−0.14	−0.14	2029.30	4.95	−0.06	−0.08		
^{285}Md	2039.59	5.17	−0.13	−0.13	2036.62	5.20	0.00	−0.00		
^{287}Md	2045.92	4.98	−0.10	−0.11	2042.50	6.76	−0.03	−0.05		
^{289}Md	2052.01	4.88	−0.09	−0.11	2049.26	4.90	0.08	0.11		
^{291}Md	2058.37	3.88	0.09	0.11	2056.03	4.05	0.12	0.14		

be directly related to the spherical shell closure of $N=184$. The whole trend of the variation of the deformation parameters in Bk isotopes is similar to that in lighter elements. There is a prolate deformation at the beginning of an open shell, and this prolate deformation decreases after the middle of a shell. Then an oblate deformation appears and it tends to zero at the closure of a shell. It seems that the predicted variation of nuclear deformation by the RMF model is consistent with the known facts of nuclear deformation along the isotopic chains of lighter elements.

For Es isotopes the RMF model predicts that nuclear deformation is prolate from ^{239}Es ($N=140$) to ^{267}Es ($N=168$) (see Table II). The deformation parameter is approximately $\beta_p \approx \beta_n = 0.27$–$0.31$ around $N=152$, and it qualitatively agrees with experimental facts [11,12,35]. From ^{269}Es ($N=170$) to ^{281}Es ($N=182$) there is a small oblate deformation, and it decreases with the increase of neutron number. The nuclei around ^{283}Es ($N=184$) are approximately spherical.

It is seen from the variation of deformation that there may be a spherical closure at $N=184$ for Bk and Es isotopes. A conclusion on the shell closure can be drawn from the variation of α-decay energies or that of two-neutron separation energy on an isotopic chain. The calculated α decay energy is listed in Tables I and II, and the variation of the α-decay energy is also drawn in Fig. 3. A plot of two-neutron separation energy versus neutron number is given in Fig. 4. It is seen from Tables I and II that the calculated α-decay energies are close to the experimental ones for known nuclei. The good agreement between the theoretical decay energy and the experimental one is also seen in Fig. 3. For unknown nuclei, there is a sudden increase of α-decay energies at $N=186$ (^{271}Bk and ^{283}Es). This indicates that $N=184$ is approximately a spherical magic number for Bk and Es isotopes. This is confirmed by the plot of the two-neutron separation energy versus neutron number, where a maximum appears at $N=184$ for Bk isotopes (see Fig. 4). Actually we also calculate the properties of $N=184$ isotones and find that the $N=184$ isotones with low proton number ($80<Z\leqslant 100$) are approximately spherical and they have a smaller α-decay energy than neighboring nuclei (or a larger two-neutron separation energy). This means that $N=184$ is approximately a spherical magic number for nuclei with proton number $80<Z\leqslant 100$.

B. Binding energies, α-decay energies, and deformations of odd-*A* Md and Lr isotopes

The numerical results of Md and Lr isotopes with TMA and NLZ2 are listed in Tables III and IV. Table III are the results of Md isotopes where the range of neutron number is 140–190. The theoretical binding energies with two sets of

TABLE IV. The binding energies, α-decay energies, and deformations of odd-even Lr isotopes with TMA and NLZ2. Columns 2–5 are the RMF results with TMA, and columns 6–9 are those with NLZ2.

Nuclei	B (MeV)	Q_α	β_n	β_p	B (MeV)	Q_α	β_n	β_p	B(Expt.) (MeV)	Q_α(Expt.)
^{247}Lr	1829.23	9.70	0.23	0.24	1826.09	9.35	0.29	0.31		
^{249}Lr	1845.33	9.28	0.24	0.25	1842.66	8.63	0.30	0.31		
^{251}Lr	1860.77	9.06	0.25	0.25	1858.69	8.06	0.30	0.32		
^{253}Lr	1875.66	8.90	0.25	0.26	1873.72	7.99	0.30	0.32	1872.73#	8.99#
^{255}Lr	1890.18	8.42	0.26	0.27	1887.72	7.90	0.30	0.32	1887.52	8.36
^{257}Lr	1904.14	8.10	0.26	0.27	1901.03	7.51	0.30	0.31	1901.02#	9.01
^{259}Lr	1916.71	8.48	0.26	0.27	1913.98	6.91	0.30	0.31	1913.96#	8.67#
^{261}Lr	1928.90	7.92	0.21	0.22	1926.56	6.45	0.29	0.30	1926.42#	8.20#
^{263}Lr	1940.70	7.38	0.26	0.27	1938.35	6.48	0.29	0.30	1938.41#	7.73#
^{265}Lr	1952.03	6.96	0.21	0.21	1949.53	6.39	0.28	0.29	1950.12#	7.37#
^{267}Lr	1963.09	6.59	0.20	0.21	1959.56	6.84	0.27	0.29		
^{269}Lr	1973.53	6.55	0.19	0.19	1968.94	7.02	0.26	0.28		
^{271}Lr	1983.47	6.59	0.17	0.17	1978.51	6.55	0.33	0.33		
^{273}Lr	1993.18	6.37	0.14	0.15	1987.72	6.46	0.20	0.22		
^{275}Lr	2003.13	6.00	−0.16	−0.16	1997.55	5.72	−0.18	−0.18		
^{277}Lr	2013.47	5.79	−0.17	−0.17	2007.63	5.76	−0.16	−0.16		
^{279}Lr	2022.57	6.33	−0.16	−0.16	2017.63	5.34	−0.14	−0.14		
^{281}Lr	2031.38	6.10	−0.15	−0.15	2027.33	5.19	−0.13	−0.13		
^{283}Lr	2040.10	5.70	−0.14	−0.14	2035.93	5.77	−0.14	−0.14		
^{285}Lr	2048.25	5.73	−0.14	−0.14	2044.03	5.67	−0.07	−0.08		
^{287}Lr	2055.37	6.03	−0.14	−0.14	2051.44	6.16	0.00	0.00		
^{289}Lr	2062.00	5.88	−0.11	−0.12	2058.09	6.83	0.04	0.06		
^{291}Lr	2068.75	5.47	−0.10	−0.11	2065.42	5.37	0.09	0.12		
^{293}Lr	2075.58	4.73	0.09	0.12	2072.57	4.99	0.12	0.15		

RMF forces agree well with the data of Md isotopes where the estimated value by Audi *et al.* [34] is denoted by the symbol #. The variation of average binding energies of Md and Lr isotopes with nucleon number is also drawn in Fig. 1(b). This shows again that the good agreement of binding energies between RMF model and the data is systematic. The previous discussions on binding energies of Table I hold true for Table III and we do not repeat them here. It is interesting to point out that we have to use some estimated values of the binding energies and α-decay energies from Audi *et al.* [34] in order to test the global behavior of the RMF model. This is because the experimental binding energies of heavy nuclei are very poor. We denote those estimated values with #. It is expected that those values should be reliable. For the data of α decay of ^{255}Lr, it is taken from Gan *et al.* [13].

The quadrupole deformation parameters of Md and Lr isotopes are listed in Tables III and IV. It is seen that many Md and Lr nuclei are deformed. There is a prolate deformation from ^{241}Md ($N=140$) to ^{269}Md. For ^{271}Md there appears shape coexistence. There is a small prolate deformation in ^{271}Md with TMA but there is an oblate deformation with NLZ2. From ^{273}Md to ^{283}Md there is an oblate deformation with both TMA and NLZ2. However the oblate deformation with TMA exists beyond ^{283}Md ($N=184$) for TMA, and the deformation of ^{283}Md with NLZ2 is approximately zero. Therefore there is no spherical shell structure at $N=184$ with TMA but there still exists spherical shell structure at $N=184$ with NLZ2. This conclusion is further supported by theoretical α-decay energies of Md isotopes in Table III.

The theoretical α-decay energies of Md are close to the experimental data for known nuclei. For unknown nuclei, the predicted values by two sets of RMF forces are very close in quantity. However, the variation trends of decay energies around $N=184$ are different for TMA and NLZ2. The decay energy of ^{283}Md with TMA is close to that of neighboring nuclei, and it indicates that there is no shell effect at $N=184$. The decay energy of ^{283}Md with NLZ2 is lower than that of ^{285}Md and it could indicate that there is still shell effect at $N=184$.

For Lr isotopes the conclusions on binding energies and deformations of Md isotopes are also valid for those of Lr nuclei. We do not repeat these discussions. The nuclear shell effect around $N=184$ disappears if we see the variation of α-decay energies on Lr isotopes. The α decay energy at $N=184$ is close to that of the neighboring nuclei. This conclusion will be true for slightly heavier elements such as Db or Bh.

C. Binding energies, α-decay energies, and deformations of odd-A Db and Bh isotopes

The theoretical results of Db and Bh isotopes are listed in Tables V and VI. Here most of the data in the last two columns are the estimated values. For the data of α-decay energy of ^{259}Db, it is taken from Gan *et al.* [13]. The agreement between the model and the data is very good. The

TABLE V. The binding energies, α-decay energies, and deformations of odd-even Db isotopes with TMA and NLZ2. Columns 2–5 are the RMF results with TMA, and columns 6–9 are those with NLZ2.

Nuclei	B (MeV)	Q_α	β_n	β_p	B (MeV)	Q_α	β_n	β_p	B(Expt.) (MeV)	Q_α(Expt.)
^{253}Db	1863.66	9.97	0.25	0.25	1861.86	9.10	0.30	0.32		
^{255}Db	1879.44	9.63	0.25	0.25	1877.79	9.20	0.30	0.32		
^{257}Db	1894.76	9.20	0.25	0.26	1892.80	9.22	0.30	0.32	1891.72#	9.31#
^{259}Db	1909.54	8.94	0.26	0.26	1907.05	8.97	0.30	0.31	1906.12	9.47
^{261}Db	1923.30	9.14	0.26	0.27	1920.89	8.44	0.29	0.31	1920.04#	9.27#
^{263}Db	1936.37	8.64	0.26	0.27	1934.31	7.96	0.29	0.30	1933.22#	9.03#
^{265}Db	1949.20	8.00	0.26	0.27	1946.99	7.87	0.28	0.30	1946.06#	8.66#
^{267}Db	1961.16	7.84	0.21	0.22	1959.04	7.61	0.28	0.29		
^{269}Db	1972.95	7.38	0.21	0.21	1969.67	8.15	0.27	0.29		
^{271}Db	1984.12	7.27	0.19	0.20	1979.52	8.34	0.26	0.28		
^{273}Db	1994.38	7.45	0.18	0.18	1989.52	7.71	0.32	0.33		
^{275}Db	2004.37	7.40	0.16	0.16	1999.29	7.52	0.19	0.20		
^{277}Db	2014.55	6.93	0.13	0.14	2009.58	6.45	0.16	0.18		
^{279}Db	2024.97	6.46	−0.17	−0.17	2019.55	6.30	0.15	0.16		
^{281}Db	2034.63	7.14	−0.17	−0.16	2029.67	6.25	−0.14	−0.14		
^{283}Db	2043.93	6.94	−0.15	−0.15	2039.89	6.04	−0.13	−0.13		
^{285}Db	2053.19	6.49	−0.14	−0.14	2049.05	6.58	−0.14	−0.15		
^{287}Db	2061.99	6.41	−0.14	−0.15	2057.70	6.53	−0.07	−0.08		
^{289}Db	2069.79	6.77	−0.15	−0.15	2065.45	6.87	−0.08	−0.09		
^{291}Db	2077.05	6.63	−0.16	−0.16	2072.97	6.77	−0.10	−0.12		
^{293}Db	2084.19	6.11	−0.10	−0.11	2080.63	5.75	0.54	0.54		
^{295}Db	2091.53	5.52	0.10	0.13	2088.36	5.36	0.53	0.54		

variation of average binding energies of Db and Bh is also drawn in Fig. 2. Two sets of theoretical results in RMF model agree even for neutron-rich nuclei around $N=190$. On deformations of the isotopes of the above two elements, there exists a slight difference. The quadrupole deformation of Db isotopes with TMA is similar to that of Lr nuclei. There is a prolate deformation in lighter Db nuclei and there is an oblate deformation in slightly heavier Db nuclei in

TABLE VI. The binding energies, α-decay energies, and deformations of odd-even Bh isotopes with TMA and NLZ2. Columns 2–5 are the RMF results with TMA, and columns 6–9 are those with NLZ2.

Nuclei	B (MeV)	Q_α	β_n	β_p	B (MeV)	Q_α	β_n	β_p	B(Expt.) (MeV)	Q_α(Expt.)
^{259}Bh	1898.01	9.74	0.25	0.26	1895.29	10.80	0.30	0.31		
^{261}Bh	1913.79	9.27	0.25	0.26	1910.46	10.64	0.29	0.30	1909.46#	10.56
^{263}Bh	1928.26	9.58	0.25	0.25	1925.23	10.13	0.29	0.30	1924.18#	10.23#
^{265}Bh	1942.18	9.42	0.25	0.25	1939.56	9.62	0.28	0.30	1938.37#	9.97#
^{267}Bh	1955.67	9.00	0.22	0.23	1953.30	9.32	0.28	0.29		
^{269}Bh	1968.73	8.77	0.22	0.22	1966.36	8.93	0.27	0.29		
^{271}Bh	1981.17	8.29	0.21	0.21	1977.75	9.59	0.27	0.28		
^{273}Bh	1992.91	8.34	0.20	0.20	1988.34	9.63	0.25	0.27		
^{275}Bh	2003.78	8.65	0.19	0.19	1998.94	8.88	0.21	0.22		
^{277}Bh	2014.14	8.55	0.18	0.18	2009.72	8.10	0.19	0.20		
^{279}Bh	2024.62	8.06	0.14	0.14	2020.48	7.11	0.17	0.18		
^{281}Bh	2035.16	7.69	−0.17	−0.17	2031.01	6.87	0.15	0.16		
^{283}Bh	2045.40	7.90	−0.17	−0.16	2041.34	6.51	0.48	0.47		
^{285}Bh	2055.19	7.74	−0.15	−0.15	2051.48	6.49	0.50	0.49		
^{287}Bh	2064.97	7.26	−0.14	−0.14	2061.17	7.02	0.51	0.50		
^{289}Bh	2074.34	7.15	−0.14	−0.14	2070.31	7.04	−0.06	−0.07		
^{291}Bh	2083.10	7.20	0.49	0.49	2078.91	7.09	0.51	0.50		
^{293}Bh	2091.35	6.74	0.48	0.48	2087.38	6.38	0.51	0.50		
^{295}Bh	2099.46	5.89	0.43	0.42	2095.70	5.57	0.51	0.50		
^{297}Bh	2107.86	4.63	0.42	0.41	2103.82	5.11	0.50	0.50		

TABLE VII. The binding energies, α-decay energies, and deformations of odd-even Mt isotopes with TMA and NLZ2. Columns 2–5 are the RMF results with TMA, and columns 6–9 are those with NLZ2. The last column is the quadrupole deformation parameter of the Skyrme-Hartree-Fock model.

Nuclei	B (MeV)	Q_α	β_n	β_p	B (MeV)	Q_α	β_n	β_p	β_2 (SHF)
^{265}Mt	1931.19	10.89	0.24	0.25	1927.80	10.96	0.27	0.28	0.27
^{267}Mt	1945.86	10.69	0.24	0.24	1942.79	10.73	0.27	0.28	0.25
^{269}Mt	1960.19	10.29	0.22	0.23	1957.41	10.45	0.27	0.28	0.25
^{271}Mt	1973.99	9.99	0.21	0.22	1971.50	10.10	0.26	0.27	0.23
^{273}Mt	1987.23	9.79	0.21	0.21	1983.77	10.89	0.26	0.27	0.23
^{275}Mt	1999.76	9.71	0.20	0.20	1995.62	10.43	0.22	0.23	0.21
^{277}Mt	2011.32	9.89	0.19	0.19	2007.30	9.34	0.20	0.21	0.21
^{279}Mt	2022.31	9.77	0.18	0.18	2018.82	8.42	0.19	0.20	0.42
^{281}Mt	2033.61	8.82	0.43	0.43	2030.23	7.79	0.17	0.18	0.44
^{283}Mt	2045.22	7.70	0.44	0.44	2041.31	7.48	0.15	0.17	0.44
^{285}Mt	2056.06	7.39	0.45	0.44	2051.98	7.33	0.50	0.48	0.43
^{287}Mt	2066.31	7.39	0.45	0.44	2062.70	6.94	0.50	0.49	0.44
^{289}Mt	2076.25	7.24	0.46	0.45	2072.88	6.91	0.51	0.50	−0.04
^{291}Mt	2086.13	7.14	0.47	0.46	2082.43	7.04	0.51	0.50	0.00
^{293}Mt	2095.82	6.82	0.48	0.47	2091.61	7.00	0.51	0.50	0.00
^{295}Mt	2104.85	6.55	0.44	0.43	2100.62	6.59	0.50	0.49	0.00
^{297}Mt	2114.01	5.63	0.43	0.42	2109.46	6.22	0.49	0.49	0.00
^{299}Mt	2122.99	4.77	0.42	0.41	2118.12	5.88	0.48	0.48	0.50

RMF model with TMA force. There is no spherical shell effect for ^{289}Db ($N=184$) because its deformation is not zero in the RMF model with TMA. The variation of α-decay energy in Fig. 3 does not support that there is a magic number at $N=184$ for Db isotopes. The RMF model with NLZ2 predicts that there is a prolate deformation in the lighter Db nuclei and there is an oblate deformation in the slightly heavier Db nuclei. There is no spherical shell effect for ^{289}Db ($N=184$) because its deformation is not zero in the RMF model with NLZ2. These agree with the conclusions drawn by the TMA force. However, a superdeformed solution appears in the ground states of ^{293}Db and ^{295}Db in the RMF model with NLZ2. This is different from that with TMA. But for heavier isotopes a superdeformed solution exists for many nuclei due to shape coexistence of nuclear structure. Especially, the existence of superderformed solutions will be a common phenomenon for some superheavy nuclei. This is almost independent of the force parameters

TABLE VIII. The binding energies, α-decay energies, and deformations of odd-even $Z=111$ isotopes with TMA and NLZ2. Columns 2–5 are the RMF results with TMA, and columns 6–9 are those with NLZ2. The last column is the quadrupole deformation parameter of the Skyrme-Hartree-Fock model.

Nuclei	B (MeV)	Q_α	β_n	β_p	B (MeV)	Q_α	β_n	β_p	β_2 (SHF)
^{271}111	1962.42	11.75	0.21	0.22	1959.95	11.14	0.25	0.26	0.23
^{273}111	1977.12	11.37	0.21	0.21	1974.85	10.86	0.25	0.25	0.21
^{275}111	1991.40	10.89	0.20	0.20	1988.17	11.62	0.23	0.24	0.21
^{277}111	2005.10	10.43	0.19	0.19	2001.23	10.85	0.21	0.22	0.42
^{279}111	2017.61	10.45	0.18	0.18	2013.96	9.96	0.19	0.20	0.42
^{281}111	2029.33	10.30	0.17	0.18	2026.33	9.27	0.18	0.19	0.43
^{283}111	2041.19	9.42	0.44	0.45	2038.45	8.67	0.17	0.18	0.45
^{285}111	2053.62	8.30	0.46	0.46	2050.19	8.34	0.15	0.16	0.45
^{287}111	2064.99	8.52	0.46	0.47	2060.94	8.67	0.13	0.14	0.45
^{289}111	2075.76	8.60	0.46	0.46	2072.36	7.92	0.52	0.52	0.46
^{291}111	2086.30	8.31	0.46	0.46	2083.03	7.96	0.53	0.53	0.00
^{293}111	2096.81	7.74	0.47	0.46	2093.10	8.07	0.54	0.54	0.00
^{295}111	2107.07	7.36	0.48	0.47	2103.38	7.34	0.61	0.61	0.00
^{297}111	2116.80	7.32	0.44	0.43	2112.17	7.74	0.51	0.50	0.00
^{299}111	2126.53	6.62	0.43	0.42	2121.50	7.42	0.50	0.49	0.00
^{301}111	2136.02	6.29	0.42	0.41	2130.62	7.14	0.49	0.48	0.50

TABLE IX. The binding energies, α-decay energies, and deformations of odd-even $Z=113$ and $Z=115$ isotopes with TMA and NLZ2. Columns 2–5 are the RMF results with TMA, and columns 6–9 are those with NLZ2. The last column is the quadrupole deformation parameter of the Skyrme-Hartree-Fock model.

Nuclei	B (MeV)	Q_α	β_n	β_p	B (MeV)	Q_α	β_n	β_p	β_2 (SHF)
$^{277}113$	1993.96	11.45	0.19	0.19	1991.23	11.92	0.22	0.23	0.43
$^{279}113$	2008.64	11.06	0.18	0.19	2005.30	11.17	0.20	0.20	0.43
$^{281}113$	2022.12	11.28	0.18	0.18	2019.20	10.33	0.19	0.19	0.43
$^{283}113$	2034.64	11.28	0.17	0.17	2032.49	9.76	0.17	0.18	0.45
$^{285}113$	2047.31	10.32	0.47	0.48	2045.38	9.26	0.16	0.17	0.45
$^{287}113$	2060.70	8.79	0.47	0.48	2057.80	8.95	0.15	0.16	0.45
$^{289}113$	2072.59	9.32	0.48	0.48	2069.11	9.37	0.55	0.56	0.47
$^{291}113$	2083.83	9.46	0.48	0.49	2080.84	8.39	0.54	0.56	0.00
$^{293}113$	2094.91	9.15	0.48	0.49	2092.31	8.35	0.61	0.62	0.00
$^{295}113$	2105.99	8.62	0.49	0.49	2103.45	7.88	0.61	0.61	0.00
$^{297}113$	2116.81	8.30	0.49	0.49	2114.20	7.21	0.60	0.61	0.00
$^{299}113$	2126.91	8.47	0.47	0.47	2123.84	7.84	0.61	0.61	0.01
$^{301}113$	2137.00	8.09	0.44	0.44	2132.91	7.57	0.61	0.62	0.49
$^{303}113$	2146.94	7.88	0.42	0.42	2141.42	8.38	0.50	0.50	0.50
$^{285}115$	2037.50	12.92	0.17	0.18	2036.53	10.97	0.17	0.18	0.45
$^{287}115$	2051.88	11.06	0.48	0.50	2050.18	10.61	0.16	0.17	0.45
$^{289}115$	2066.01	9.60	0.48	0.50	2063.15	10.53	0.15	0.16	0.45
$^{291}115$	2078.58	10.43	0.49	0.50	2075.93	10.17	0.55	0.57	0.46
$^{293}115$	2090.96	9.93	−0.22	−0.22	2088.28	9.13	0.55	0.57	0.46
$^{295}115$	2102.42	9.71	0.50	0.51	2100.22	8.92	0.60	0.61	0.00
$^{297}115$	2114.15	9.07	0.51	0.51	2112.06	8.55	0.60	0.61	0.00
$^{299}115$	2125.45	8.84	0.51	0.51	2123.35	8.40	0.60	0.61	0.00
$^{301}115$	2136.01	9.10	0.55	0.55	2133.59	8.90	0.60	0.61	0.00
$^{303}115$	2146.22	8.99	0.46	0.46	2143.26	8.88	0.61	0.61	0.47
$^{305}115$	2156.45	8.86	0.42	0.42	2152.56	8.65	0.63	0.64	0.50

that were used in RMF calculations. We will also point out in the following that other models such as the deformed Skyrme-Hartree-Fock model also find the existence of superdeformed solutions for superheavy nuclei.

Now let us see the details of the superdeformed solutions in other isotopes. The results of Bh isotopes are presented in Table VI. For lighter nuclei on this chain there exists a prolate deformation in the ground state of these nuclei. For heavier Bh nuclei there is shape coexistence, and a superdeformed solution appears for some of them. This solution becomes the ground state of some nuclei. We also carry out a constraint RMF calculation and confirm the existence of this solution. $N=184$ (^{291}Bh) is not a magic number for Bh isotopes. This is clearly seen from Figs. 3 and 4. The superdeformed solution is the ground state of nuclei $^{291-297}$Bh with TMA, and the superdeformed solution is the ground state of nuclei $^{283-287,291-297}$Bh with NLZ2. Although the results with two sets of RMF forces are not exactly same on the deformation of nuclei, it is common that there exist superdeformed solutions for superheavy nuclei. The total variation of deformation parameters with nucleon number is similar for two sets of forces in the RMF model. It is expected that other forces of the RMF model show similar behavior for superheavy nuclei.

D. Binding energies, α-decay energies, and deformations of odd-A $Z=109$, 111, 113, 115 isotopes

The numerical results of $Z=109$–115 isotopes are given in Tables VII–IX. The quantities in columns 1–9 have the same meaning as those in the previous tables. The average binding energies of $Z=109$ and $Z=111$ are plotted in Fig. 2. For nuclei of these four elements the data of binding energies and α-decay energy are unknown or very few. Therefore there is no meaning to list them. Instead, we list in the last column of Tables VII–IX the quadrupole deformation parameter of deformed Skyrme-Hartree-Fock (SHF) model [36] for comparison.

It is seen from Tables VII–IX that there is prolate deformation in lighter nuclei of an isotopic chain but there is superdeformation in heavier nuclei in the RMF model. For these four isotopic chains superdeformation appears around $N=172$ in the RMF model with TMA. With NLZ2 it appears around $N=176$. This again shows that superdeformation may be common in the RMF calculations of superheavy nuclei. It is interesting to compare the RMF results of superheavy nuclei with those from deformed SHF model [36]. The quadrupole deformation parameter β_2 of the deformed SHF model is given in the last column of Tables VII–IX.

For the Mt isotopes in Table VII it is seen that the SHF model predicts prolate deformation in ligher nuclei

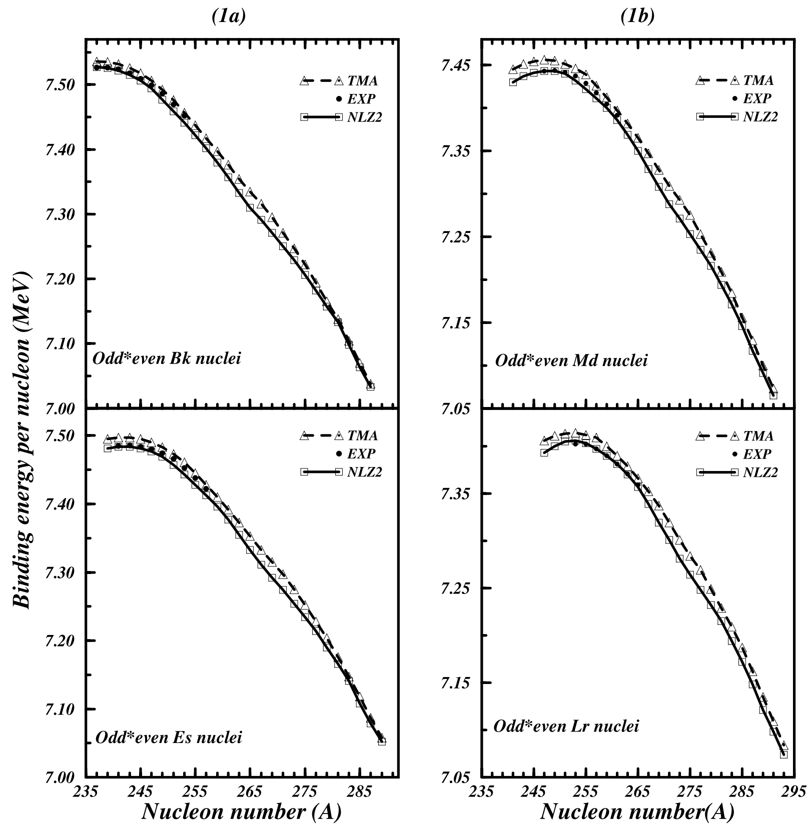

FIG. 1. The comparison of theoretical and experimental average binding energy of nucleons for nuclei with $Z=97$, 99, 101, 103. The two sets of theoretical results are connected by solid curves.

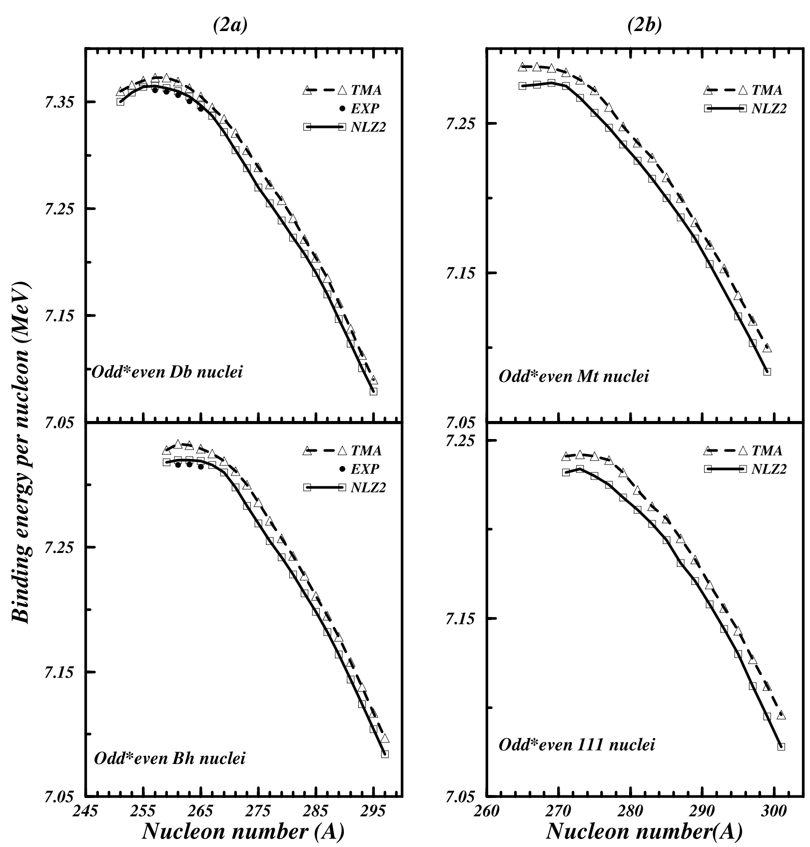

FIG. 2. The comparison of theoretical and experimental average binding energy of nucleons for nuclei with $Z=105$, 107, 109, 111. The two sets of theoretical results are connected by solid curves.

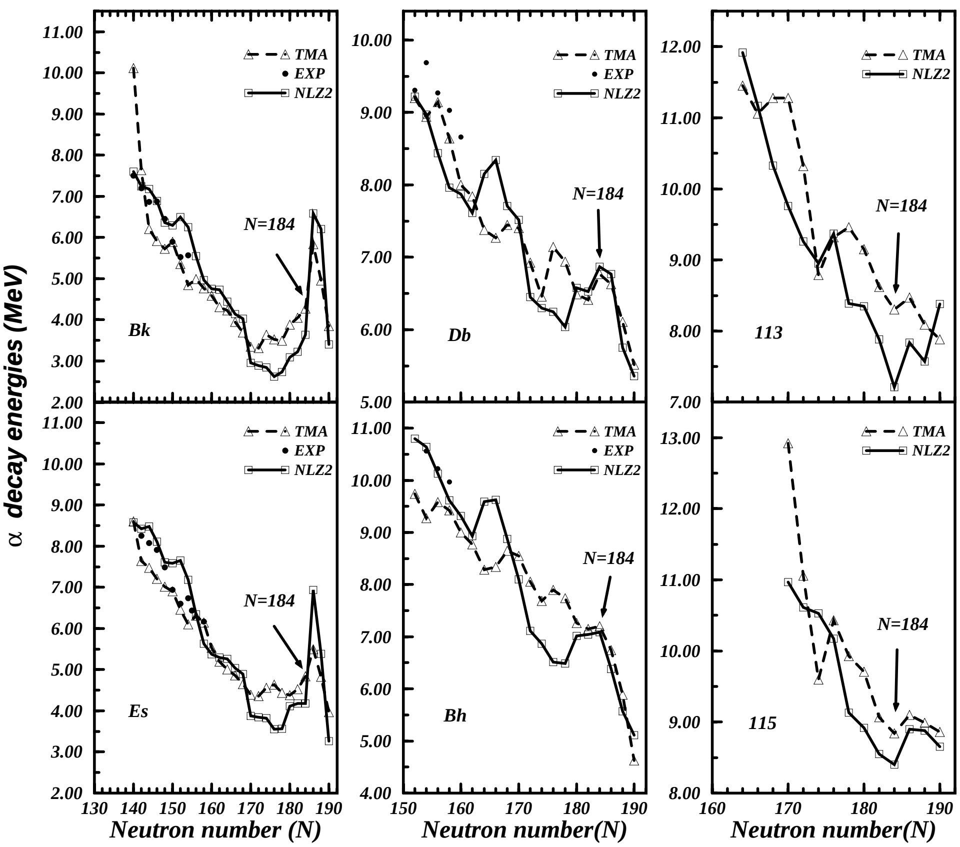

FIG. 3. The variation of α-decay energy with neutron number on Bk, Es, Db, Bh, $Z=113$ and $Z=115$ isotopic chains. The left part of Fig. 3 is for Bk and Es elements. The middle one is that of Db and Bh elements. The right part is for $Z=113$ and $Z=115$ elements. The two sets of theoretical results are connected by dashed and solid curves. The experimental decay energy is denoted by black points.

($^{265-277}$Mt). It predicts that there exists superdeformation in heavier nuclei ($^{279-299}$Mt). The superdeformation in the SHF model appears around $N=170$. This number is very close to the number $N=172$ in the RMF model with TMA. For a quantitative comparison of deformation between two models it is seen that the quadrupole deformation parameter of $^{265-277}$Mt in SHF model is $\beta_2=0.27$–0.21, and this is very close to that of RMF model, $\beta_2=0.28$–0.19. The deformation parameter of $^{279-287,299}$Mt in SHF model is $\beta_2=0.42$–0.44 in superdeformed cases. This is also close to the value of $^{285-299}$Mt $\beta_2=0.41$–0.50 in the RMF model. A difference between two models is that the superdeformed solution exists until $N=190$ in RMF model but it does not correspond to the ground state of $^{289-297}$Mt in the SHF model.

For $Z=111$ isotopic chain (Table VIII), the SHF model predicts that there is a prolate deformation in lighter nuclei $^{271-275}$111 and there is a superdeformed solution in heavier nuclei $^{277-289}$111. These are in qualitative agreement with those in the RMF model. The nuclei $^{291-289}$111 are approximately spherical in the SHF model, and this fact is different from the results of the RMF model.

For $Z=113$ and 115 isotopes (Table IX) there is superdeformation in many nuclei in the SHF model, and this is in qualitative agreement with that in the RMF model. But the nuclei around $N=184$ are spherical in the SHF model, and those are superdeformed in the RMF model. Although ^{297}113 and ^{299}115 are spherical in the SHF model, there is no shell structure according to two-neutron separation energies of the SHF model. For the RMF model there is a small deformed subshell structure at ^{297}113 and ^{299}115 ($N=184$) according to the α-decay energy in Table IX (also see Fig. 3). This is seen more clearly from Fig. 4 where the variation of two-neutron separation energy with neutron number is drawn for $Z=115$ isotopic chain. A decrease of the separation energy appears at $N=186$, and it corresponds to a deformed subshell closure. Therefore the spherical magic number $N=184$ exists in the RMF model for lighter elements ($Z\leqslant 100$), but it disappears for heavier elements ($100<Z<112$) due to deformation. For $Z=113$ and $Z=115$ isotopic chains, $N=184$ may become a deformed magic number due to superdeformation.

III. SUMMARY

We have calculated the ground state properties of odd-Z superheavy nuclei in the mass range of $Z=97$–115 and $N=140$–190 in the RMF model with TMA and NLZ2 forces. Calculations show that the theoretical binding energies and α-decay energies of the RMF model agree very well with the experimental data. This study demonstrates that the RMF model is very stable even for nuclei with high neutron number $N=190$ because two sets of RMF results agree well for the unknown mass range. For known heavy nuclei around $Z=100$ and $N=152$, nuclear deformation predicted by the RMF model agrees with the present data. For $N=184$ isotones there are varying structures for different proton numbers in the RMF model. The RMF model predicts that $N=184$ is a magic number for $Z\leqslant 100$, and the $N=184$ iso-

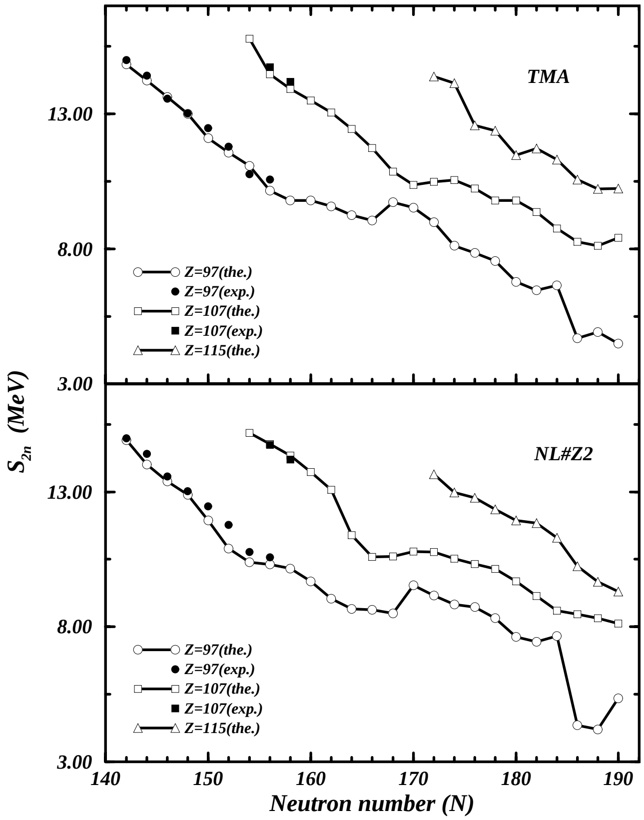

FIG. 4. The variation of two-neutron separation energy with neutron number on Bk ($Z=97$), Bh ($Z=107$), and $Z=115$ isotopic chains. The upper part of Fig. 4 is the RMF result with TMA. The lower part is that with NLZ2. The theoretical results of an isotopic chain are connected by solid curves. The experimental separation energy is denoted by black points.

tones with $Z\leqslant 100$ are approximately spherical. The $N=184$ isotones with $100<Z<110$ are deformed and the magic number $N=184$ disappears. For $Z=113$ and $Z=115$ isotopic chains, $N=184$ corresponds to a deformed subshell. It is found by the RMF model that there is superdeformation in some superheavy nuclei due to shape coexistence of nuclear structure. The deformation parameters of the RMF model for unknown mass range are very close to those from the deformed Skyrme-Hartree-Fock model [36] for some superheavy nuclei. Importantly, there is also superdeformation for some superheavy nuclei in the SHF model, and the magnitude of the superdeformation is close to that of RMF model for some superheavy nuclei. This shows that two self-consistent mean-field models are in agreement in the global behavior of deformation.

Therefore deformation is important for superheavy nuclei and it should be included in the calculations of ground state properties of these nuclei. The deformation plays a crucial role for the possible existence of shell structure. This paper presents a systematic calculation on odd-Z superheavy nuclei with the RMF model, and is also a significant extension of our previous study to unknown mass range. The complete comparison with various experimental data such as binding energies, α-decay energies, and deformations is useful to test the reliability of the RMF model. The predicted binding energies, α-decay energies, and deformation of unknown mass range will be useful for future experimental study of superheavy nuclei.

ACKNOWLEDGMENTS

Z. Ren thanks Professor T. Otsuka, Professor H. Toki, Professor H. Q. Zhang, Professor Z. Qin, Professor Z. G. Gan, and Professor J. S. Guo for kindly communicating him new progress related to superheavy nuclei. This work was supported by the National Natural Science Foundation of China (Grant No. 10125521), by the 973 National Major State Basic Research and Development of China (Grant No. G2000077400), by the CAS Knowledge Innovation Project, Grant No. KJCX2-SW-N02, and by the fund of the Education Ministry of China for the training of Ph.D. students under Contract No. 20010284036.

[1] S. Hofmann, V. Ninov, F.P. Heßberger, P. Armbruster, H. Folger, G. Münzenberg, H.J. Schött, A.G. Popeko, A.V. Yeremin, A.N. Andreyev, S. Saro, R. Janik, and M. Leino, Z. Phys. A **350**, 277 (1995).

[2] S. Hofmann, V. Ninov, F.P. Heßberger, P. Armbruster, H. Folger, G. Münzenberg, H.J. Schött, A.G. Popeko, A.V. Yeremin, A.N. Andreyev, S. Saro, R. Janik, and M.S. Leino, Z. Phys. A **350**, 281 (1995).

[3] S. Hofmann, V. Ninov, F.P. Heßberger, P. Armbruster, H. Folger, G. Münzenberg, H.J. Schött, A.G. Popeko, A.V. Yeremin, S. Saro, R. Janik, and M. Leino, Z. Phys. A **354**, 229 (1996).

[4] S. Hofmann and G. Münzenberg, Rev. Mod. Phys. **72**, 733 (2000).

[5] Yu.Ts. Oganessian, A.V. Yeremin, A.G. Popeko, S.L. Bogomolov, G.V. Buklanov, M.L. Chelnokov, V.I. Chepigin, B.N. Gikal, V.A. Gorshkov, G.G. Gulbekian, M.G. Itkis, A.P. Kabachenko, A.Y. Lavrentev, O.N. Malyshev, J. Rohac, R.N. Sagaidak, S. Hofmann, S. Saro, G. Giardina, and K. Morita, Nature (London) **400**, 242 (1999).

[6] Yu.Ts. Oganessian, V.K. Utyonkov, Yu.V. Lobanov, F.Sh. Abdullin, A.N. Polyakov, I.V. Shirokovsky, Yu.S. Tsyganov, G.G. Gulbekian, S.L. Bogomolov, B.N. Gikal, A.N. Mezentsev, S. Iliev, V.G. Subbotin, A.M. Sukhov, G.V. Buklanov, K. Subotic, and M.G. Itkis, Phys. Rev. Lett. **83**, 3154 (1999).

[7] Yu.Ts. Oganessian, V.K. Utyonkov, Yu.V. Lobanov, F.Sh. Abdullin, A.N. Polyakov, I.V. Shirokovsky, Yu.S. Tsyganov, G.G. Gulbekian, S.L. Bogomolov, B.N. Gikal, A.N. Mezentsev, S. Iliev, V.G. Subbotin, A.M. Sukhov, O.V. Ivanov, G.V. Buklanov, K. Subotic, M.G. Itkis, K.J. Moody, J.F. Wild, N.J. Stoyer, M.A. Stoyer, and R.W. Lougheed, Phys. Rev. C **62**, 041604(R) (2000).

[8] Yu.Ts. Oganessian, V.K. Utyonkov, Yu.V. Lobanov, F.Sh. Abdullin, A.N. Polyakov, I.V. Shirokovsky, Yu.S. Tsyganov, G.G.

Gulbekian, S.L. Bogomolov, B.N. Gikal, A.N. Mezentsev, S. Iliev, V.G. Subbotin, A.M. Sukhov, O.V. Ivanov, G.V. Buklanov, K. Subotic, M.G. Itkis, K.J. Moody, J.F. Wild, N.J. Stoyer, M.A. Stoyer, R.W. Lougheed, C.A. Laue, Ye.A. Karelin, and A.N. Tatarinov, Phys. Rev. C **63**, 011301(R) (2001).

[9] Ch.E. Düllman, W. Brüchle, R. Dressler, K. Eberhardt, B. Eichler, R. Eichler, H.W. Gäggeler, T.N. Ginter, F. Glaus, K.E. Gregorich, D.C. Hoffman, E. Jäger, D.T. Jost, U.W. Kirbach, D.M. Lee, H. Nitsche, J.B. Patin, V. Pershina, D. Piguet, Z. Qin, M. Schädel, B. Schausten, E. Schimpf, H.J. Schött, S. Soverna, R. Sudowe, P. Thörle, S.N. Timokhin, N. Trautmann, A. Türler, A. Vahle, G. Wirth, A.B. Yakushev, and P.M. Zielinski, Nature (London) **418**, 859 (2002).

[10] S. Hofmann, F.P. Heßberger, D. Ackermann, S. Antalic, P. Cagarda, S. Cwiok, B. Kindler, J. Kojouharova, B. Lommel, R. Mann, G. Münzenberg, A.G. Popeko, S. Saro, H.J. Schött, and A.V. Yeremin, Eur. Phys. J. A **10**, 5 (2001).

[11] P. Reiter, T.L. Khoo, C.J. Lister, D. Seweryniak, I. Ahmad, M. Alcorta, M.P. Carpenter, J.A. Cizewski, C.N. Davids, and G. Gervais, Phys. Rev. Lett. **82**, 509 (1999).

[12] P.A. Butler, R.D. Humphreys, P.T. Greenless, R.D. Herzberg, D.G. Jenkins, G.D. Jones, H. Kankaanpä, H. Kettunen, P. Rahkila, C. Scholey, J. Uusitalo, N. Amzal, J.E. Bastin, P.M.T. Brew, K. Eskola, J. Gerl, N.J. Hammond, K. Hauschild, K. Helariutta, F.P. Heßberger, A. Hürstel, P.M. Jones, R. Julin, S. Juutinen, A. Keenan, T.L. Khoo, W. Korten, P. Kuusiniemi, Y.Le. Coz, M. Leino, A.P. Leppänen, M. Muikku, P. Nieminen, S.W. Odegard, T. Page, J. Pakarinen, P. Reiter, G. Sletten, Ch. Theisen, and H.J. Wollersheim, Phys. Rev. Lett. **89**, 202501 (2002).

[13] Z.G. Gan, Z. Qin, H.M. Fan, X.G. Lei, Y.B. Xu, J.J. He, H.Y. Liu, X.L. Wu, J.S. Guo, X.H. Zhou, S.G. Yuan, and G.M. Jin, Eur. Phys. J. A **10**, 21 (2001).

[14] W.Q. Shen, J. Albinski, A. Gobbi, S. Gralla, K.D. Hildenbrand, N. Herrmann, J. Kuzminski, W.F.J. Müller, H. Stelzer, J. Tōke, B.B. Back, S. Bjørnholm, and S.P. Sørensen, Phys. Rev. C **36**, 115 (1987).

[15] I. Muntian, Z. Patyk, and A. Sobiczwski, Phys. Lett. B **500**, 241 (2001).

[16] P. Möller, J.R. Nix, and K.L. Kratz, At. Data Nucl. Data Tables **66**, 131 (1997).

[17] W.D. Myers and W.J. Swiatecki, Phys. Rev. C **58**, 3368 (1998).

[18] Zhongzhou Ren and H. Toki, Nucl. Phys. **A689**, 691 (2001).

[19] K. Rutz, M. Bender, T. Buervenich, T. Schilling, P.G. Reinhard, J.A. Maruhn, and W. Greiner, Phys. Rev. C **56**, 238 (1997).

[20] Zhongzhou Ren, Phys. Rev. C **65**, 051304(R) (2002).

[21] Zhongzhou Ren, Fei Tai, and Ding-Han Chen, Phys. Rev. C **66**, 064306 (2002).

[22] M. Bender, K. Rutz, P.G. Reinhard, J.A. Maruhn, and W. Greiner, Phys. Rev. C **60**, 034304 (1999).

[23] B.D. Serot and J.D. Walecka, Adv. Nucl. Phys. **16**, 1 (1986).

[24] P.G. Reinhard, D.J. Dean, W. Nazarewicz, J. Dobaczewski, J.A. Maruhn, and M.R. Strayer, Phys. Rev. C **60**, 014316 (1999).

[25] Y.K. Gambhir, P. Ring, and A. Thimet, Ann. Phys. (N.Y.) **198**, 132 (1990).

[26] S. Marcos, N. Van Giai, and L.N. Savushkin, Nucl. Phys. **A549**, 143 (1992).

[27] D. Hirata, H. Toki, I. Tanihata, and P. Ring, Phys. Lett. B **314**, 168 (1993).

[28] Zhongzhou Ren, Z.Y. Zhu, Y.H. Cai, and Gongou Xu, Phys. Lett. B **380**, 241 (1996).

[29] T.R. Werner, J.A. Sheikh, W. Nazarewicz, M.R. Strayer, A.S. Umar, and M. Misu, Phys. Lett. B **333**, 303 (1994).

[30] Zhongzhou Ren, Amand Faessler, and A. Bobyk, Phys. Rev. C **57**, 2752 (1998).

[31] B.Q. Chen, Z.Y. Ma, F. Gruemmer, and S. Krewald, Phys. Lett. B **455**, 13 (1999).

[32] G.A. Lalazissis, M.M. Sharma, P. Ring, and Y.K. Gambhir, Nucl. Phys. **A608**, 202 (1996).

[33] S.K. Patra, C.L. Wu, C.R. Praharaj, and R.K. Gupta, Nucl. Phys. **A651**, 117 (1999).

[34] G. Audi, O. Bersilion, J. Blachot, and A.H. Wapstra, Nucl. Phys. **A624**, 1 (1997).

[35] S. Raman *et al.*, At. Data Nucl. Data Tables **36**, 1 (1987).

[36] S. Goriely, F. Tondeur, and J.M. Pearson, At. Data Nucl. Data Tables **77**, 311 (2001).